

## EMBROIDERED SPLIT RING RESONATOR ANTENNA

J. Hao<sup>1</sup>, A. Leblanc<sup>2</sup>, L. Burgnies<sup>1,3</sup>, A. Djouadi<sup>1</sup>, X. Tao<sup>2</sup>, C. Cochrane<sup>2</sup>, F. Rault<sup>2</sup>,  
V. Koncar<sup>2</sup>, É. Lheurette<sup>1</sup>

<sup>1</sup> Univ. Lille, CNRS, Centrale Lille, ISEN, Univ. Polytech. H-d-F, UMR 8520 - IEMN, F-59000 Lille, France

<sup>2</sup> ENSAIT, GEMTEX - Laboratoire de Génie et Matériaux Textiles, F-59000 Lille, France

<sup>3</sup> Université du Littoral Côte d'Opale, rue Ferdinand Buisson, F-62228 Calais

cedric.cochrane@ensait.fr

### ABSTRACT

A textile integrated antenna made of a dipole and split ring resonators (SRR) produced by embroidery is under consideration. A size reduction of the antenna was achieved by means of a resonance of the SRRs and connection loss was lessened by using a copper wire for the dipole. Embroidery for SRR fabrication with metallic yarn was studied in order to achieve a minimal distance between concentric rings, and an antenna was designed and produced. The manufactured antenna showed a double band operation at 1.8 and 2.2 GHz with a measured gain of 0 and -3.1 dBi, respectively.

**Key Words:** textile antenna, body-worn antenna, metamaterial antenna, split ring resonator, embroidery

### 1. INTRODUCTION

Improving the performance of antennas is currently sought in literature. With this goal, metamaterials are often involved because they allow a size reduction of the antenna by means of their resonant feature [1], [2]. An electrically small antenna (ESA) can be produced by a metamaterial-inspired resonator strongly coupled to a radiative element (electric dipole or patch antenna for instance). In such an antenna, the metamaterial resonator has to be selected in order to ensure an efficient coupling with the radiative element. Commonly, an ESA can be produced by a split ring resonator (SRR) magnetically coupled to an electric dipole [1], [2]. Such an SRR can be considered to improve other antenna performances as well. We can mention a bandwidth and a gain enhancement [3], a reduction of the side lobe radiation [4], or the production of a multi-band operation [5]. Generally, these antennas are fabricated in printed circuit board and for body-worn applications a better integration in textile is required. Electronics integration in textile is a broad topic in which antennas show specific constraints as a change of the radiation pattern under curvature, or a behavior dependence on the permittivity of the textile substrate. Therefore, textile antennas and textile materials for electromagnetic applications are commonly studied by several groups [6]-[12]. On the other hand, the connection of textile antennas is a more global problem and it has to be kept in mind during the design of new realistic products.

In this paper, we show experimental results of a textile metamaterial antenna produced by embroidery. The antenna consists of SRRs embroidered with a metallic yarn and an S-shaped dipole made of a copper wire held on textile by means of dielectric yarn embroidery. The antenna was first designed by means of parametric simulations performed with commercial electromagnetic software. Then, the antenna was produced after a preliminary optimization step of the embroidery machine. Finally, the manufactured antenna was characterized in terms of impedance matching and radiation pattern. Each part is described in the next sections.

## 2. DESIGN

A scheme of the antenna is shown in inset of Fig. 1a. An S-shaped electric dipole is coupled to two circular SRRs and it is connected at the center position. A circular shape was selected both for an easier fabrication of SRRs and in order to limit conductive loss. Moreover, a lower resonance frequency can be achieved for an S-shaped dipole of diameter  $D$ , compared with a straight dipole of length  $2xD$  yielding a better integration. For the targeted applications at 2.45 GHz, the frequency shift is around 1 GHz. The entire geometrical parameters act on the antenna performance and some parametric studies were performed for designing antenna. Such parametric studies were calculated with commercial electromagnetic software and main results are summed-up below.

### 2.1 Gap between concentric rings and distance between the dipole and the SRRs

The operation principle of the antenna is based on a resonance of the SRRs and a size reduction is achieved by increasing the capacitance between concentric rings. Therefore, a small gap between rings is required. Similarly, the distance between the dipole and the SRRs has to be smaller as possible in order to increase the coupling between the radiative element and the resonators. The reflection coefficient at the antenna input is plotted in Fig. 1a with the gap between rings as a parameter. The reflection coefficient was calculated for a dipole diameter  $D = 19$  mm and an outer ring diameter  $d_2 = 14$  mm. Then, the diameter of the inner ring was varied in order to achieve a gap between rings  $g = 0.25$  to 1.5 mm. Other parameters were a strip-width of 1 mm for rings, a slot of 1.5 mm for each ring, and a dipole-width of 0.2 mm. In Fig. 1a, the reflection shows two resonances (dips) for each  $g$  value. For  $g = 0.25$  mm, the dip at 1.9 GHz can be associated to the SRRs resonance whereas the dipole resonance is concerned with the second one. By increasing  $g$ , the SRRs resonance increases because the capacitance between concentric rings decreases. We can observe a balanced operating mode for  $g = 0.5$  mm with two dips at very close frequency and a reflection lower than -15 dB. Such a low value for  $S_{11}$  corresponds to an impedance matching of the antenna to  $50 \Omega$ . For  $g = 1$  and 1.5 mm, the SRRs resonate at a higher frequency than the dipole and a bad impedance matching is observed with only a reflection of -9 and -5 dB at 2.9 and 3.1 GHz, respectively. Also, we can note a quasi-invariant resonance frequency for the dipole at 2.3 GHz for  $g \geq 1$  mm.

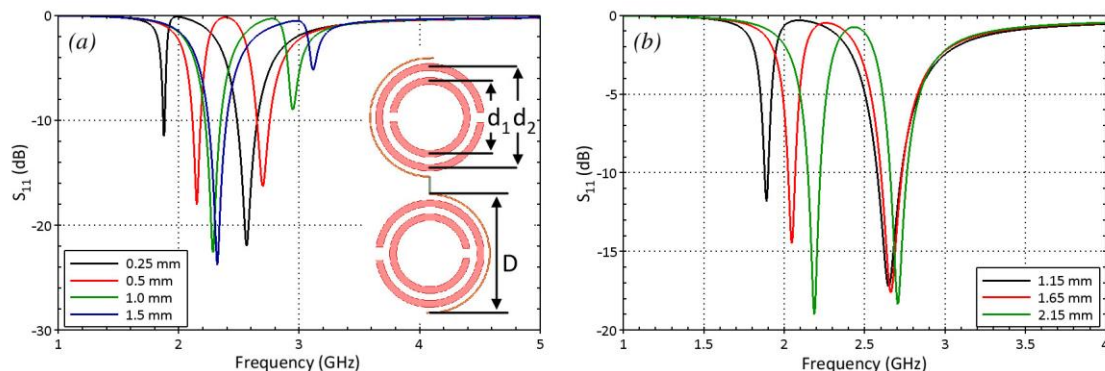


**Figure 1.** Reflection coefficient with the gap between rings as a parameter (a) and with the distance between the dipole and the SRRs as a parameter (b).

A similar study was performed with the distance between the dipole and the SRRs as a parameter. For the reflection coefficient plotted in Fig. 1b, the diameters of the two concentric rings  $d_1$  and  $d_2$  were simultaneously varied whereas the gap between them and the dipole

diameter were kept constant (i.e.  $g = 0.5$  mm and  $D = 19$  mm). When the distance increases, we can see a frequency shift of the first dip due to the size reduction of rings which produce a resonance of the SRRs at higher frequency. The observation of a dip at the SRRs resonance points out that the coupling between the dipole and the resonators still exists whatever the distance. However, the expected decrease of the coupling by moving the SRRs away from the dipole is not observed in Fig. 1b. Finally, we can note that the resonance of the dipole at around 2.6 GHz is slightly changed with only a frequency shift of 4%.

## 2.2 Conductivity of the SRRs

The SRRs were produced by means of embroidery of a metallic yarn. Such a yarn has to be enough flexible for embroidery and often it consists of conductive multifilament. Then, conductive filaments are twisted producing the electrical continuity of the yarn. But the conductivity of the yarn is often low compared with the conductivity of bulk metal as copper. Moreover, after embroidery it is commonly observed filament breakages which will more reduce the conductivity of the embroidered patterns. Conductivity has a direct incidence on the quality factor of the resonators and consecutively on the antenna performance.

The reflection coefficient and the impedance calculated at the input of the antenna are plotted respectively in Fig. 2a and Fig. 2b with the conductivity of the SRRs as a parameter. Other geometric parameters were  $D = 19$  mm,  $d_2 = 14$  mm, and  $g = 1.25$  mm, and the value of the conductivity  $\sigma_{max} = 1.44 \cdot 10^5$  S/m corresponds to the measured value in DC of the considered yarn for fabrication.

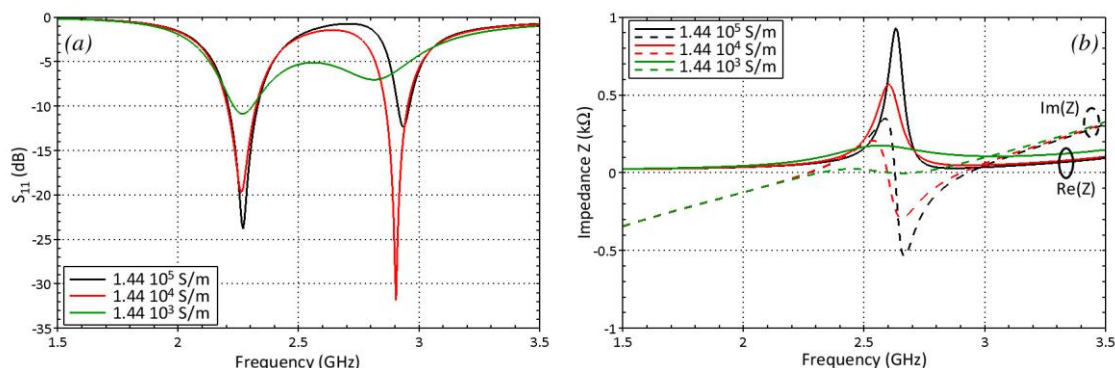


**Figure 2.** Reflection coefficient (a) and impedance (b) calculated at the input of the antenna with the conductivity of the SRRs as a parameter.

We can see that the first reflection dip is still narrow up to  $\sigma_{max}/10$  and tends to vanish for  $\sigma_{max}/100$ . This trend can be understood by observing the real part of the impedance plotted in Fig. 2b. By decreasing the conductivity, the maximum value of the real part of the impedance at the resonance frequency of the SRRs decreases and the imaginary part of the impedance around the resonance becomes flat for  $\sigma_{max}/100$ . Therefore, the inductive reactance introduced by the SRRs under their resonance frequency is no more enough to compensate the capacitive reactance of the dipole and the antenna tends to behave as a simple dipole without SRRs.

## 2.3 Length of the dipole

After fabrication, the antenna behavior can be adjusted by changing the length of the dipole. The Fig. 3a and Fig. 3b show the reflection coefficient and the impedance calculated in the input of the antenna respectively. As illustrated in inset of Fig. 3a, the case  $\theta = 0^\circ$  corresponds to the previous S-shaped dipole (half ring dipole) whereas the dipole is lengthened of 2x5 mm

for  $\theta = 30^\circ$ . For these simulations, all the geometric parameters of the SRRs ( $D = 19$  mm,  $d_2 = 14$  mm, and  $g = 1.25$  mm) were kept constant and then the resonance frequency of the SRRs is invariant around 2.6 GHz as observed in Fig. 3b.

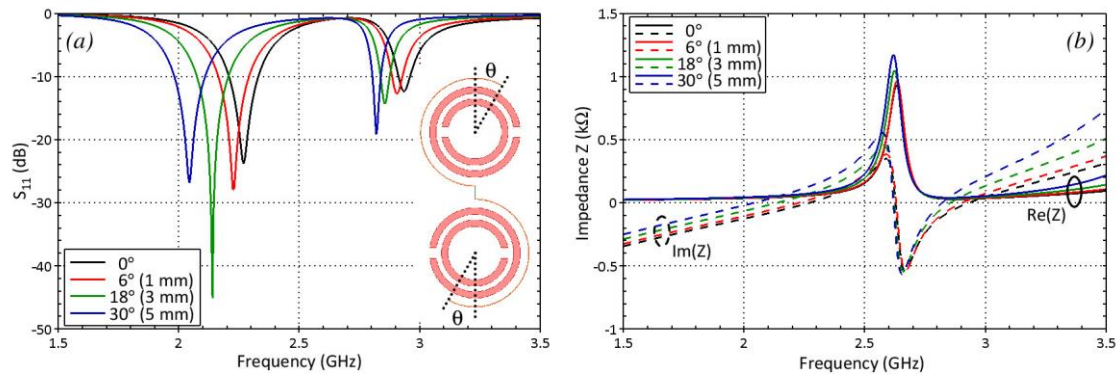


**Figure 3.** Reflection coefficient (a) and impedance (b) calculated at the input of the antenna with an elongation of the dipole as a parameter.

The shift of the first dip down to lower frequency observed in Fig 3a stems from the decrease of the resonance frequency of the dipole. When the dipole is longer, the imaginary part of the impedance due to the dipole is higher producing a frequency shift of the impedance matching condition of the antenna and consecutively of the first reflection dip.

### 3. FABRICATION

Previously to the production of the designed antenna, a technological study was led on embroidery of the SRRs. The goal was to define the smaller gap  $g$  which can be reached by avoiding any risk of electrical connection between rings. Indeed, such a connection should destroy the resonance of the SRRs. The SRRs were embroidered on a computerized embroidery machine (JF 0211-495 from ZSK) by using a silver-based conductive yarn from Statex Company (Shieldex® Twisted Yarns 117/17 dtex 2-Ply). The conductive yarn was used for upper threading whereas a polyester dielectric yarn was used for lower threading. The conductive yarn consists of continuous conductive multifilament and filament breakages were observed after embroidery fabrication. Filament breakages produce a hairiness which might short-circuit concentric rings and consecutively might destroy the resonance of the SRRs. It was concluded that disconnected rings can be achieved with a gap higher than 1 mm, and  $g = 1$  mm was finally targeted for the production of the embroidered SRRs.

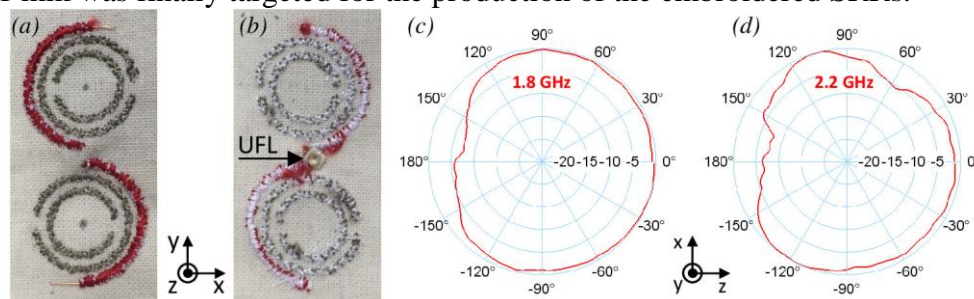


**Figure 4.** Front (a) and back (b) side of the antenna produced by embroidery. Radiation pattern measured at 1.8 GHz (c) and 2.2 GHz (d).

On the other hand, the S-shaped dipole was produced by a copper wire of diameter 0.2 mm which can be easily soldered for connection. The copper wire was longer than the designed length of the dipole, and it was cut after fabrication in order to adjust during measurements the dipole resonance as observed in Fig. 3. Fig. 4 shows the front and the back side of the

fabricated antenna. We can see an UFL connector soldered in the middle of the dipole in the back side while a 5 mm-length copper wire exceeding the embroidered part of the dipole is shown in the front side. After fabrication, all sizes were measured  $D = 18.4$  mm,  $d_2 = 14$  mm and  $g = 1.3$  mm.

#### 4. CHARACTERIZATION

The fabricated antenna was first electromagnetically characterized by means of a Vector Network Analyzer (VNA) previously calibrated (SOLT calibration) at the input plane of the UFL connector. With such a calibration, the experimental impedance of the antenna can be calculated from the measured reflection coefficient without supplemental complex post-processed de-embedding. The measured reflection and the impedance of the antenna are plotted in Fig. 5a and Fig. 5b, respectively. We can see that the antenna operates in a balanced mode with two dips at 1.8 and 2.2 GHz and a reflection lower than -33 dB. This low reflection value reflects a good impedance matching on both sides of the resonance of the SRRs observed at around 2 GHz in Fig. 5b. By comparing the results plotted in Fig. 5b for experiments and results plotted in Fig. 2b for simulation, the low value of the impedance measured at the resonance ( $150 \Omega$ ) points out a low conductivity of the rings.

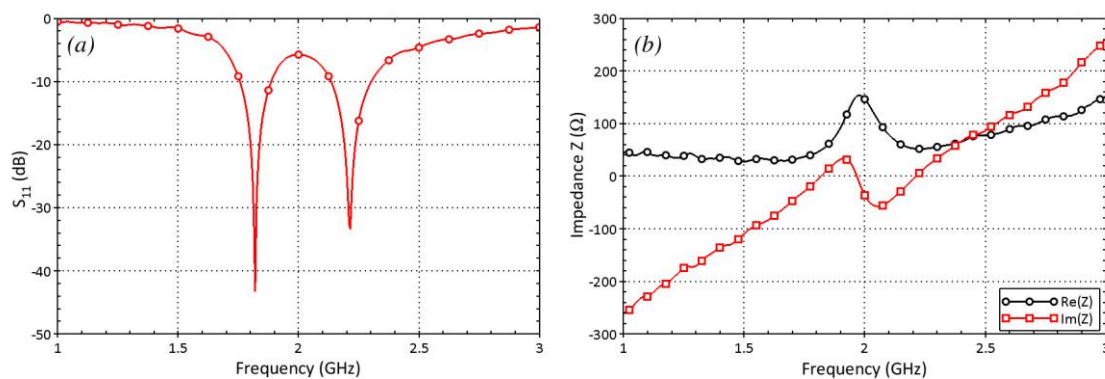


**Figure 5.** Measured reflection (a) and measured impedance (b) of the fabricated antenna.

The radiation pattern and the gain of the antenna were measured in an anechoic chamber. A double ridge guide horn antenna SAS 571 from A. H. Systems Inc. was used as a receiving antenna for the radiation pattern and as reference antennas for the gain measurement. The normalized radiation pattern measured at 1.8 and 2.2 GHz is plotted in Fig. 4c and Fig. 4d, respectively. As the antenna was supply in the back side, a disturbance of the radiation pattern is observed between  $-90^\circ$  and  $+90^\circ$ . Otherwise, the radiation pattern is similar to the radiation pattern of a simple electric dipole antenna without SRRs. Finally, the measured gain was 0 dBi and -3.1 dBi at 1.8 and 2.2 GHz, respectively.

#### 5. CONCLUSION

A textile antenna based on split ring resonators (SRRs) has been designed, fabricated and characterized. By means of electromagnetic simulations, a parametric study showed that the resonance frequency of the SRRs and of the dipole can be tuned by adjusting the gap between rings and the length of the dipole, respectively. The dependence of the conductivity of SRRs on the antenna response was also analyzed. It was shown that the resonance of the SRRs tends to vanish by decreasing the conductivity. The antenna was manufactured by embroidery in order to facilitate both integration on textile and connection. After a preliminary fabrication



study, a 1 mm-gap between rings was selected for avoiding any electrical contact between rings which might arise from the hairiness of the embroidered metallic yarn. Experiments showed a double band operation of the antenna stemming from the resonance of the SRRs with a radiation pattern looking as the radiation pattern of a simple dipole antenna without SRRs.

## 6. ACKNOWLEDGMENTS

This work was supported financially by the Fonds Européen de Développement Régional/Met steun van het Europees Fonds voor Regionale Ontwikkeling in the framework of the European Interreg V France-Wallonie-Vlaanderen project named Luminoptex.

## 7. REFERENCES

1. K. B. Alici and E. Ozbay, Electrically small split ring resonator antennas, *Journal of Applied Physics*, 2007, Vol. 101, No. 8, 083104.
2. Y. Dong and T. Itoh, Metamaterial-Based Antennas, *Proc. of IEEE*, 2012, Vol. 100, No. 7, 2271–2285.
3. R. Su, P. Gao, R. Wang, and P. Wang, High-gain broadside dipole planar AMC antenna for 60 GHz applications, *Electronics Letters*, 2018, Vol. 54, No. 7, 407–408.
4. X. Chen, Y. Ge, and T. S. Bird, Reduction of sidelobe radiations of the standard pyramidal horn using a thin metamaterial lens, *Electronics Letters*, 2016, Vol. 52, No. 24, 1973–1974.
5. D. K. Ntaikos, N. K. Bourgis, and T. V. Yioultis, Metamaterial-Based Electrically Small Multiband Planar Monopole Antennas, *IEEE Antennas Wireless and Propagation Letters*, 2011, Vol. 10, 963–966.
6. K. Kamardin, M. K. Abd Rahim, N. A. Samsuri, M. E. B. Jalil, and I. H. Idris, Textile Artificial Magnetic Conductor Waveguide Jacket for on-Body Transmission Enhancement, *Progress In Electromagnetics Research*, 2013, Vol. 54, 45–68.
7. Z. Wang, L. Z. Lee, D. Psychoudakis, and J. L. Volakis, Embroidered Multiband Body-Worn Antenna for GSM/PCS/WLAN Communications, *IEEE Transactions on Antennas and Propagation*, 2014, Vol. 62, No. 6, 3321–3329.
8. F. X. Liu, Z. Xu, D. C. Ranasinghe, and C. Fumeaux, Textile Folded Half-Mode Substrate-Integrated Cavity Antenna, *IEEE Antennas and Wireless Propagation Letters*, 2016, Vol. 15, 1693–1697.
9. L. Burgnies, C. Cochrane, F. Rault, V. Sadaune, É Lheurette, V. Koncar, and D. Lippens, Experimental phase-advance in woven textile metasurface, *Applied Physics Letters*, 2015, Vol. 107, No. 20, 203505.
10. R. Seager, S. Zhang, A. Chauraya, W. Whittow, Y. Vardaxoglou, T. Acti, and T. Dias, Effect of the fabrication parameters on the performance of embroidered antennas, *Antennas Propagation IET Microwaves*, 2013, Vol. 7, No. 14, 1174–1181.
11. N. F. M. Aun, P. J. Soh, A. A. Al-Hadi, M. F. Jamlos, G. A. E. Vandenbosch, and D. Schreurs, Revolutionizing Wearables for 5G: 5G Technologies: Recent Developments and Future Perspectives for Wearable Devices and Antennas, *IEEE Microwave Magazine*, 2017, Vol. 18, No. 3, pp. 108–124.
12. L. Burgnies, C. Huppé, G. Ducournau, C. Cochrane, F. Rault, V. Koncar, and É Lheurette, High-Pass Sub-mmWave Filtering by Woven Textile Metamaterials, *IEEE Transactions on Terahertz Science and Technology*, 2018, Vol. 8, No. 4, 427–433.